



# Triterpenoid modulation of IL-17 and Nrf-2 expression ameliorates neuroinflammation and promotes remyelination in autoimmune encephalomyelitis

SUBJECT AREAS:

PATHOLOGY

IMMUNOLOGY

NEURODEGENERATION

GENE REGULATION

Received  
27 October 2011

Accepted  
18 November 2011

Published  
19 December 2011

Correspondence and  
requests for materials  
should be addressed to  
J.J.L. (John.Letterio@  
UHhospitals.org)

Tej K. Pareek<sup>1</sup>, Abdelmadjid Belkadi<sup>2</sup>, Sashi Kesavapany<sup>3</sup>, Anita Zaremba<sup>2</sup>, Sook L. Loh<sup>3</sup>, Lianhua Bai<sup>2</sup>, Mark L. Cohen<sup>4</sup>, Colin Meyer<sup>5</sup>, Karen T. Liby<sup>6</sup>, Robert H. Miller<sup>2</sup>, Michael B. Sporn<sup>6</sup> & John J. Letterio<sup>1</sup>

<sup>1</sup>Department of Pediatrics/Division of Pediatric Hematology-Oncology, University Hospitals Case Medical Center and The Case Comprehensive Cancer Center, Case Western Reserve University, Cleveland, OH 44106, <sup>2</sup>Centers for Stem Cells and Regenerative Medicine, Translational Neuroscience, Department of Neurosciences, Case Western Reserve University, School of Medicine, Ohio 44106, Cleveland, <sup>3</sup>Department of Biochemistry, Neurobiology Program, Yong Loo Lin School of Medicine, National University of Singapore, Singapore, 117597, <sup>4</sup>Department of Pathology, Case Western Reserve University, OH 44106, <sup>5</sup>Reata Pharmaceuticals Inc., Irving, TX 75063, <sup>6</sup>Department of Pharmacology and Toxicology, Dartmouth Medical School, Hanover, NH 03755.

**Inflammatory cytokines and endogenous anti-oxidants are variables affecting disease progression in multiple sclerosis (MS). Here we demonstrate the dual capacity of triterpenoids to simultaneously repress production of IL-17 and other pro-inflammatory mediators while exerting neuroprotective effects directly through Nrf2-dependent induction of anti-oxidant genes. Derivatives of the natural triterpene oleanolic acid, namely CDDO-trifluoroethyl-amide (CDDO-TFEA), completely suppressed disease in a murine model of MS, experimental autoimmune encephalomyelitis (EAE), by inhibiting Th1 and Th17 mRNA and cytokine production. Encephalitogenic T cells recovered from treated mice were hypo-responsive to myelin antigen and failed to adoptively transfer the disease. Microarray analyses showed significant suppression of pro-inflammatory transcripts with concomitant induction of anti-inflammatory genes including Ptgds and Hsd11b1. Finally, triterpenoids induced oligodendrocyte maturation *in vitro* and enhanced myelin repair in an LPC-induced non-inflammatory model of demyelination *in vivo*. These results demonstrate the unique potential of triterpenoid derivatives for the treatment of neuroinflammatory disorders such as MS.**

The dynamic regulation of cytoprotective genes in response to inflammatory mediators contributes to the relapsing-remitting nature of multiple sclerosis (MS)<sup>1</sup>. In murine models of MS, initiation of disease requires induction of a Th17 T cell response with disease manifestations ultimately resulting from activated macrophages which phagocytose myelin and contribute to degeneration of myelin sheaths, oligodendrocytes and axons<sup>2</sup>. Activated monocytes and macrophages produce inflammatory mediators, including nitric oxide and reactive oxygen species (ROS), which contribute to the development and progression of the disease<sup>3,4</sup>. Generation of ROS in brain parenchyma contributes to lesion persistence by mediating oligodendroglial damage and axonal injury<sup>5,6</sup>, and reduced serum levels of antioxidants have been observed in patients with MS<sup>7</sup>.

The central nervous system is endowed with several protective mechanisms consisting of enzymatic and non-enzymatic antioxidants whose expression is regulated through the transcription factor nuclear factor-E2-related factor (Nrf2) and the antioxidant response element (ARE). In humans with MS, enhanced expression of Nrf2/ARE-regulated antioxidants in the brain is indicative of the response to oxidative stress, and in mice disruption of Nrf2 gene expression (Nrf2<sup>-/-</sup> mice) leads to exacerbation of clinical and pathological symptoms of experimental autoimmune encephalomyelitis (EAE)<sup>8</sup>. Nrf2<sup>-/-</sup> mice are also hypersensitive to LPS-induced neuroinflammation<sup>9</sup> and Nrf2 is reported to be involved in maintaining CNS myelin<sup>10</sup>. To date, over 200 Nrf2/ARE-driven genes involved in detoxification and antioxidant defense have been identified, out of which superoxide dismutases (SOD), glutathione peroxidases, GPxs<sup>11</sup>, catalases<sup>4,12,13</sup>, and hemoxygenases-1 (Hmox-1)<sup>14,15</sup> are all modulated during MS.



The families of natural and synthetic triterpenoids have recently emerged as potent regulators of the Nrf2/ARE pathway. Triterpenoids represent a broad category of molecules ubiquitously present in the plant kingdom<sup>16,17</sup>, and used widely in Asian medicine (usually in the form of herbal extracts)<sup>18</sup>. Among these natural triterpenoids, the natural pentacyclic triterpene oleanolic acid (OA) displays numerous biological properties with therapeutic potential<sup>18,19</sup>. Both OA and herbal extracts containing OA are known for their immunomodulatory properties<sup>20</sup> and have been shown to reduce clinical pathology associated with neuroinflammation and EAE<sup>21,22</sup>.

Oleanolic acid has served as the platform for synthesis of several novel triterpenoids, including 2-cyano-3,12-dioxooleana-1,9(11)-dien-28-oic acid methyl ester (CDDO-Me) which is currently in Phase III clinical trials in patients with diabetic nephropathy<sup>23,24</sup>. In preclinical studies, CDDO-methyl amide (CDDO-MA) was shown to exert neuroprotective effects through potent activation of the Nrf2/ARE pathway and is neuroprotective in preclinical model systems, including a transgenic model of Alzheimer's disease<sup>25</sup>. Further derivatization of CDDO to yield an imidazolide (CDDO-Im), an ethyl amide, (CDDO-EA), or a trifluoroethyl amide (CDDO-TFEA), resulted in significantly increased biological activity<sup>26</sup>, and enhanced capacity to cross the blood brain barrier (BBB)<sup>27</sup>.

In this study we reveal the mechanisms mediating neuroprotective effects of three CDDO derivatives CDDO-Me, CDDO-EA and CDDO-TFEA in the treatment of EAE. Daily systemic administration of these compounds alone significantly alleviates the clinical symptoms of disease. We show that CDDO-TFEA not only induces Nrf2 expression and signaling both in affected CNS tissue as well as in peripheral lymphocytes, but also leads to global suppression of inflammatory response genes in mice with EAE and suppression of disease associated cytokines, particularly interleukin-17 (IL-17). Lastly, CDDO-TFEA protects against non-inflammatory lysophosphatidyl choline (LPC)-induced demyelination suggesting a direct action of this molecule on myelin preservation and repair. These results reveal the potency and unique mechanisms through which

novel synthetic triterpenoids, specifically CDDO derivatives, suppress disease progression in the setting of inflammatory neurodegenerative disease.

## Results

**CDDO derivatives promote complete resolution of EAE.** To investigate the efficacy of selected synthetic triterpenoids (Fig. 1A), mice were immunized with either MOG 35–55 (C57BL/6 mice) or PLP (139–151) (Balb/C mice) and received systemic administration of either CDDO-Me, CDDO-EA, or CDDO-TFEA after the onset of disease. Administration of triterpenoids every alternate day for 10 days significantly improved survival (Fig. 1B) and led to complete abrogation of clinical symptoms within the first two weeks of treatment, regardless of disease score at the onset of treatment (Fig. 1C). Recrudescence of disease symptoms was significantly delayed after treatment with CDDO-TFEA, when compared to CDDO-Me (Fig. S1-A) and CDDO-EA (Fig. S1-B). Re-exposure of these mice to the same molecule resulted in complete suppression of clinical symptoms in all treatment groups. The severity of symptoms at disease relapse was low and survival was greater than 90% for mice treated with either the ethyl-amide or trifluoroethylamide derivatives. The beneficial effects of CDDO-TFEA were reproducible in the remitting relapsing model of PLP (139–151)-induced EAE (Fig. 1D). The effect of these small molecules on EAE disease progression may involve a combination of suppressive activity on the peripheral immune system and direct neuroprotective effects in the CNS. The former is supported by our observation that lymphocytes collected from mice immunized with MOG (35–55) and subsequently exposed to CDDO-TFEA completely failed to adoptively transfer disease to untreated mice (Fig. S2).

**CDDO-TFEA attenuates CNS inflammation and demyelination in mice with EAE.** To assess the effects of CDDO-TFEA and other derivatives on EAE-associated CNS pathology, lumbar spinal cord and brain stem were obtained from mice either at the peak of disease

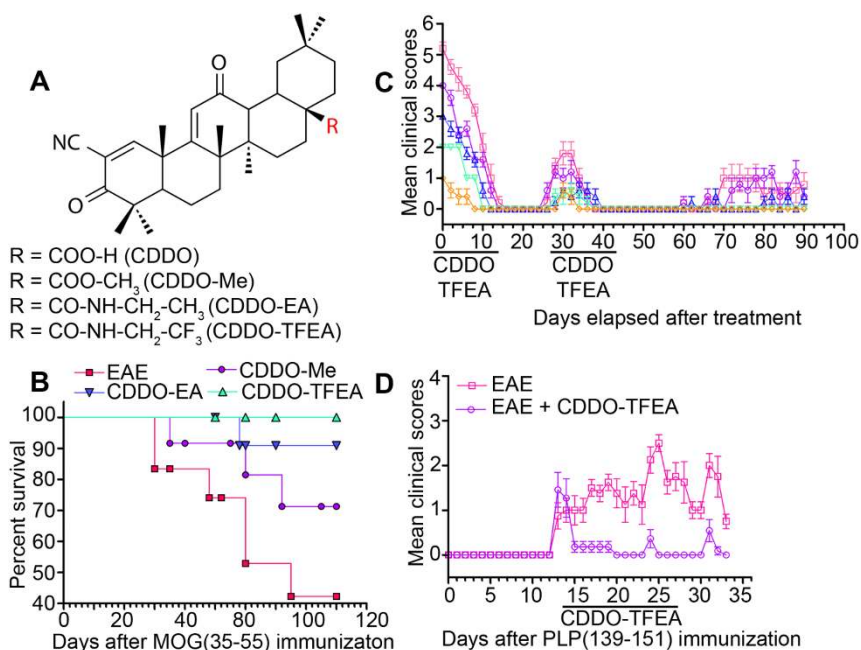


**Figure 1** | Systemic administration of CDDO derivatives ameliorates the severity of EAE. (A) Chemical structure of the parent molecule, CDDO, and its derivatives used in this study. (B) Survival of mice was recorded (Kaplan-Meier survival curve) within 3 months of MOG (35–55) immunization. (C) C57BL/6 mice were pooled at different clinical scores and CDDO-TFEA was administered by i.p. injections (as described in methods section) on alternate days at the indicated time points; a specific clinical score was assigned to each mouse at 48 hr intervals and these scores are depicted as mean clinical scores. (D) SJL mice were immunized with PLP (139–151) and treated with CDDO-TFEA on alternate days during the indicated time points. All data are presented as the mean  $\pm$  S.E.M. (n = 10–12 mice in each group).



severity or at a point when disease scores approached baseline. Independent histological analysis of brain stem (Fig. S3) and spinal cord demonstrated reduced inflammation (Fig. 2A–C & 2M) and minimal demyelination (Fig. 2D–F & 2N), in CDDO-TFEA-treated animals when compared with the untreated control group. There was a significant reduction in the number of F4/80 (macrophage and microglia; Fig. 2G–I) and myeloperoxidase (neutrophil, Fig. 2J–L) positive cells in the lumbar spinal cord of mice treated with CDDO-TFEA. These data support a conclusion that suppression of immune and inflammatory cell populations is one mechanism underlying the response to synthetic triterpenoids in EAE.

**Treatment with CDDO-TFEA diminishes inflammatory cytokine levels.** Our laboratory and others have shown direct suppressive effects of triterpenoids on immune cell activation and on receptor-mediated activation of signaling intermediates including Stat3 and NFκB<sup>28,29</sup>. To determine whether triterpenoid suppression of CNS infiltration by immune cells in mice with EAE was linked to suppression of the immune response in the periphery, we first analyzed serum and supernatants of cultured peripheral blood lymphocytes harvested from mice with EAE and re-stimulated *ex vivo* in the presence or absence of CDDO-TFEA (Fig. 3A–G). A significant reduction in Th1 and Th17 cytokines (i.e. IL6, IL17, IFNγ, TNFα and GMCSF) was observed while IL-2 production was not altered significantly. Lymphocytes collected from spleen and inguinal lymph nodes of mice 21 days after MOG (35–55) injection secreted several cytokines when restimulated with MOG (35–55) peptide *ex vivo*, but production of IL2, IL4, IL6, IL17, TNF-α, IFN-γ and GMCSF was significantly lower in lymphocytes harvested from mice treated with CDDO-TFEA. When these data were normalized for cell proliferation (to account for effects of CDDO-TFEA on cell growth) the differences in IL17 and GMCSF production remained highly significant.

**CDDO-TFEA suppresses antigen-specific lymphocyte responses and modulates Hmox-1 and iNOS protein expression.** The data presented thus far suggest that triterpenoids may suppress EAE through direct effects on immune cell activation and function. We hypothesized that CDDO-TFEA might impair development of an antigen-specific memory response to MOG (35–55) through direct suppression of T cell activation or cytokine driven proliferative expansion. Here we show that CDDO-TFEA treatment significantly inhibited the responses to CD3/CD28 and IL7 both alone and in combination (Fig. S4). Interleukin-7 (IL7) is a non-redundant cytokine essential for T cell survival and development and T cell memory<sup>30</sup>. Patients suffering with MS have a higher level of IL7 and IL7R-alpha in the cerebrospinal fluid compared with patients suffering from other non-inflammatory neurological disorders<sup>31</sup>. CDDO-TFEA significantly suppressed IL-7 stimulated *in vitro* proliferation of both quiescent and activated T cells isolated from spleen and lymph nodes of mice immunized with MOG (Fig. S4). We assessed the *ex vivo* responsiveness of lymphocytes isolated from lymph nodes and spleen of either a) control mice, b) MOG(35–55)-immunized mice with symptoms of EAE or c) MOG(35–55)-immunized mice following treatment with CDDO-TFEA. Lymphocytes derived from lymph nodes of symptomatic mice restimulated with MOG (35–55) *in vitro* had a more than 5-fold greater proliferative response relative to control lymphocytes, but this response was significantly diminished in cultures of lymphocytes isolated from mice treated with CDDO-TFEA *in vivo*. In either case, the *in vitro* treatment of these cells with CDDO-TFEA completely blocked proliferation in response to MOG (35–55) (Fig. 4A). These data demonstrate a direct suppression of the lymphocyte proliferative response to antigen and IL7 stimulation by CDDO-TFEA and related triterpenoids.

Triterpenoids have also been shown to control inflammation by suppressing expression of inducible nitric oxide synthase (iNOS) in

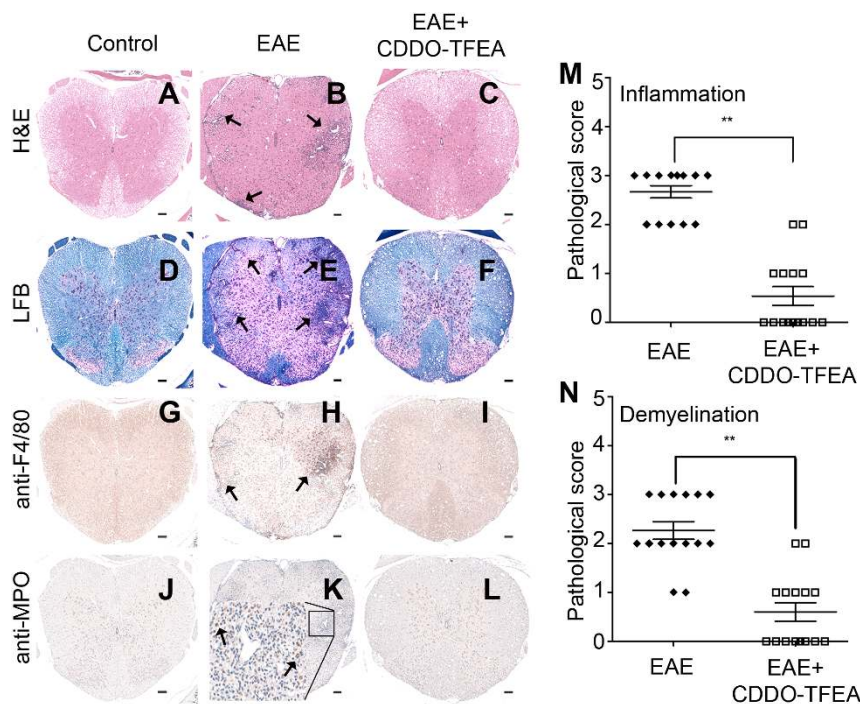


**Figure 2 | Decreased inflammation and preservation of myelin content after CDDO-TFEA treatment.** Mice were sacrificed after MOG (35–55) immunization either at the peak of clinical symptoms or at a clinical score of zero and after respective treatments with either vehicle control or CDDO-TFEA and CNS tissues were subjected to histopathological analysis. Representative sections of lumbar spinal cord (A–L) from control mice with clinical signs of EAE or from mice treated with CDDO-TFEA were stained with hematoxylin and eosin to assess inflammation (A–C), with Luxol fast blue to assess myelin content (D–F), with F4/80 to stain macrophages and microglia (G–I) and with myeloperoxidase (MPO) to stain neutrophils (J–L). Arrows indicate inflammatory cellular infiltrates (B), demyelinated areas (E) and macrophage and neutrophil infiltrates (H & K). A pathologist blinded to subject identity scored sections taken from each animal for (M) inflammation and (N) demyelination on the scale of 0 to 3 (Scale bars, 100μm). \*\*, P, 0.01, Student's t test.

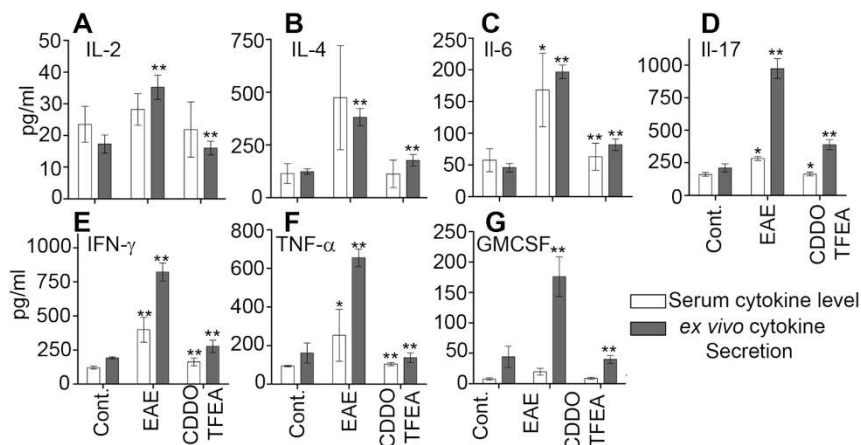


**Figure 3 | CDDO-TFEA treatment suppressed production of key inflammatory cytokines by lymphocytes during EAE.** Serum was collected from mice, including controls, mice with EAE (at clinical score 5) and mice with EAE following treatment with CDDO-derivatives both at the peak of disease severity and after they reached a clinical score 0. Production of cytokines from peripheral lymphocytes obtained from these mice was determined after culturing them for 72 hrs *ex vivo*. ELISA was performed to detect cytokine levels of IL-2 (A), IL-4 (B), IL-6 (C), IL-17 (D), IFN $\gamma$  (E), TNF- $\alpha$  (F) and GMCSF (G). All data are presented as the mean  $\pm$  SEM ( $n = 6$ ). \*\*, P, 0.01, \*, P, 0.05, Student's t test.

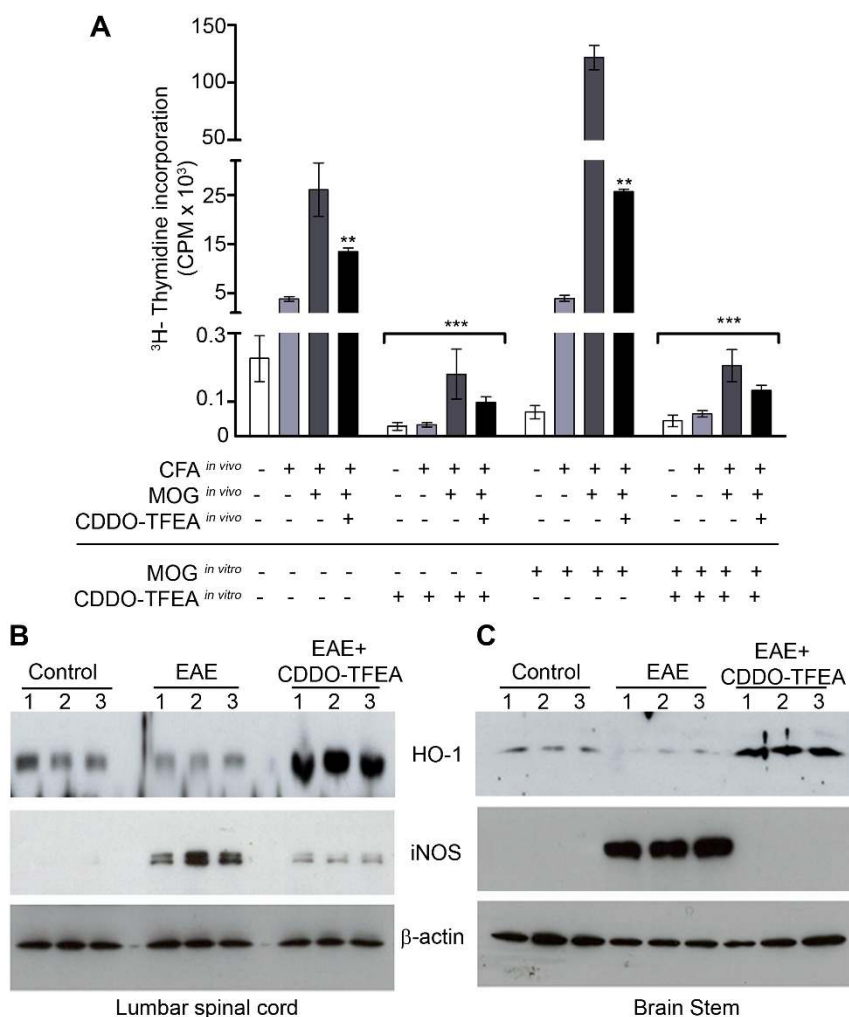


**Figure 4 | CDDO-TFEA inhibits lymphocyte proliferation and modulates iNOS and Hmox-1 protein expression in the CNS of affected mice.** (A) Lymphocytes were collected from control mice, mice with EAE (at clinical score 5) or from mice with EAE following treatment with CDDO-TFEA (at clinical score 0) and cultured for 72 hrs in the presence or absence of MOG (35–55), with or without CDDO-TFEA. During last 16 hrs, <sup>3</sup>H-thymidine was added to cultures and the incorporated amount of <sup>3</sup>H-thymidine in cells was measured as CPM. Protein lysates were prepared from lumbar spinal cord (B) and brain stem (C) of control mice, mice with EAE (at clinical score 5) or mice with EAE following CDDO-TFEA treatment (at clinical score 0) and subjected to Western blot analysis to check iNOS and Hmox-1 protein levels. Equal loading of samples was confirmed by actin immunodetection. Data is presented as the mean  $\pm$  SEM ( $n = 6$ ). \*\*\*, P, 0.001, \*\*, P, 0.01, Student's t test.



macrophages. CNS levels of iNOS increase over the course of EAE<sup>32–35</sup>, resulting in prolonged exposure to nitric oxide<sup>36</sup> which is cytotoxic<sup>37</sup> and promotes inflammation<sup>38</sup>. We found elevated levels of iNOS present in the lumbar spinal cord (Fig. 4B) and brain stem (Fig. 4C) of mice with EAE that were reduced significantly after CDDO-TFEA treatment. When the same tissues were evaluated for the expression of Hmox-1, we observed a reciprocal relationship. Prior reports have shown a link between hemin-induced Hmox-1 expression and reduced clinical severity of EAE in rats, whereas tin mesoporphyrin, a well-known inhibitor of Hmox-1 markedly exacerbated EAE<sup>15</sup>. Moreover, induction of EAE in Hmox1<sup>-/-</sup> mice led to enhanced CNS demyelination, paralysis, and mortality<sup>39</sup>. The significant up-regulation of Hmox-1 protein in brain stem and lumbar spinal cord after CDDO-TFEA treatment suggests a possible mechanism through which this small molecule may be exerting neuroprotective effects in EAE.

**Concomitant regulation of Nrf2-dependent and inflammatory gene transcription.** The observed induction of Hmox-1 protein in CNS tissues following CDDO-TFEA exposure is consistent with the ability of the triterpenoids to activate Nrf2-dependent expression of the Hmox-1 gene. We used real-time PCR to evaluate the expression of Hmox-1 and several inflammation-related genes (including IFN- $\gamma$ , IL-17 and iNOS) in total CNS tissue (Fig. 5A–B) and in splenocytes (Fig. 5C) and in mononuclear cells isolated from the CNS (Fig. 5D) of mice with EAE. A significant increase in Nrf2 and Hmox-1 transcripts was detected in lymphocytes of mice treated with CDDO-TFEA during the course of disease (Fig. 5A–C), and in mononuclear cells isolated from the CNS (Fig. 5D). Moreover, CDDO-TFEA significantly induced Nrf2 and Hmox-1 gene expression by encephalitogenic splenocytes cultured in the presence of MOG (35–55) (Fig. 5C).

The pathogenic role of IL-17 in EAE has been substantiated by studies in mice deficient in IL-17 or the IL-17-inducing cytokine IL-23<sup>40,41</sup>. We observed complete suppression of IFN- $\gamma$  and IL-17 gene expression in total CNS tissue (Fig. 5A–B) as well as in mononuclear cells isolated from brain stem and lumbar spinal cord (Fig. 5D) after CDDO-TFEA treatment. Moreover, CDDO-TFEA significantly

reduced both IFN- $\gamma$  and IL-17 expression by lymphocytes isolated from mice immunized with MOG (35–55), when these cells were re-exposed to MOG (35–55) *in vitro* (Fig. 5C). Collectively, these data highlight the multifunctional nature of the synthetic triterpenoids and the central role of Nrf2-mediated induction of pathways that combat oxidative stress, including the Hmox-1 pathway. The data also suggest the observed triterpenoid effect involves regulation of immune cells both at the site of disease and in the periphery.

**CDDO-TFEA suppresses non-inflammatory LPC-induced demyelination.** The data presented thus far suggests that neuronal integrity is maintained by CDDO-TFEA during EAE induction. However, the question remains whether this effect of CDDO-TFEA is solely due to immune suppression or whether triterpenoids also exert direct effects on myelin stability or regeneration. To address this question we utilized the well-established non-inflammatory lysophosphatidyl choline (LPC)-induced rodent model of myelin injury. Direct injection of LPC into neural tissue produces a localized vesicular demyelination of neurons that spares axons<sup>42</sup>. In the LPC-induced demyelination paradigm, a small amount of exogenous LPC injected into the dorsal columns of the thoracic spinal cord activates membrane bound phospholipase-A<sub>2</sub> which then hydrolyzes the lecithin of myelin leading to membrane solubilization and demyelination with fully developed lesions at 2 days post-injection<sup>43</sup>. To test the efficacy of CDDO-TFEA on LPC-induced de-myelination, a total of 12 rats were subjected to LPC injection within dorsal column of spinal cord; 6 of these also received 10 nM CDDO-TFEA with LPC injection and then again at the site of injury 48 hours after LPC injection. Tissues were removed 7 days following injury and processed for immunostaining with anti-MBP antibody (for myelin), anti-GFAP antibody (for astrocytes) and anti-NG2 antibody (for oligodendrocytes).

Control mice (injected with PBS) exhibit intact myelin and a normal distribution of astrocytes (Fig. 6A–D) and oligodendrocytes (Fig. S5A–D). However, at the site of LPC injection neurons were completely demyelinated (Fig. 6G & Fig. S4G), astrocytes formed a glial scar around the demyelinated area (Fig. 6F and 6H) and oligodendrocytes were recruited around demyelinated axons (Fig. S5F and S5H).

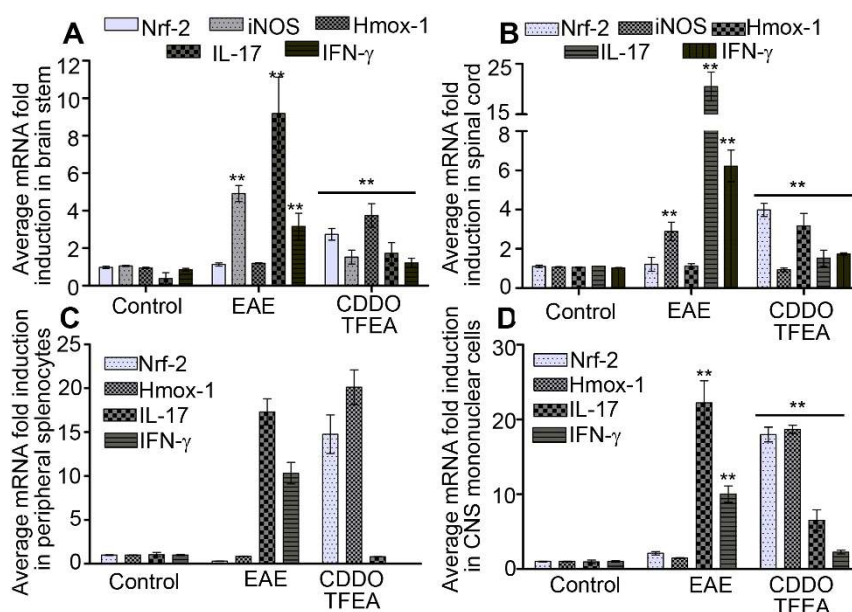


**Figure 5 | CDDO-TFEA treatment modulates both antioxidant and inflammatory gene transcription in the CNS and in peripheral lymphocytes.** Data represent the fold increase in gene expression levels as detected by quantitative PCR performed on mRNA collected from either (A–B) total CNS tissue, (C) peripheral lymphocytes or (D) mononuclear cells collected from the CNS tissues of control mice or from those with EAE (at the peak of the disease) or from mice with EAE following treatment with CDDO-TFEA (when clinical scores returned to baseline). All data are the mean  $\pm$  SEM. \*\*,  $P < 0.01$ , Student's  $t$  test.



Myelin was significantly protected in the CDDO-TFEA treated group (Fig. 6K and Fig. S5K), with a comparatively normal distribution of astrocytes and oligodendrocytes. These data were further confirmed by toluidene blue staining and electron microscopy (Fig. 6M–R). We observed completely naked axons at the site of LPC injection (Fig. 6N & 6Q) while administration of CDDO-TFEA preserved myelin at the site of LPC injection (Fig. 6O and 6R), as defined by the percentage of myelinated axons and their G ratios in the dorsal horn of the spinal cord at the site of LPC injection (Fig. 6S–T).

The data above indicate that CDDO-TFEA promotes preservation of myelin at the site of injury, but it is also possible that CDDO-TFEA may additionally promote myelin repair by facilitating oligodendrocyte maturation. To address this question, oligodendrocytes

harvested from the CNS of day E18 rat embryos and were cultured for 10 days in either the presence or absence of CDDO-TFEA. CDDO-TFEA significantly enhanced maturation of oligodendrocyte precursors as shown by expression of maturation markers A2B5 (Fig. 7A–F & 7M) and O4 (Fig. 7G–L & 7N). These data indicate that during EAE, CDDO-TFEA and related synthetic triterpenoids act as multifunctional agents, both suppressing the immune response while also acting directly on neurons to protect them from the demyelination process and to promote myelin repair.

**A unique triterpenoid-modulated transcriptome underlies the resolution of EAE.** To better characterize the triterpenoid modulated transcriptome in EAE we performed a gene microarray

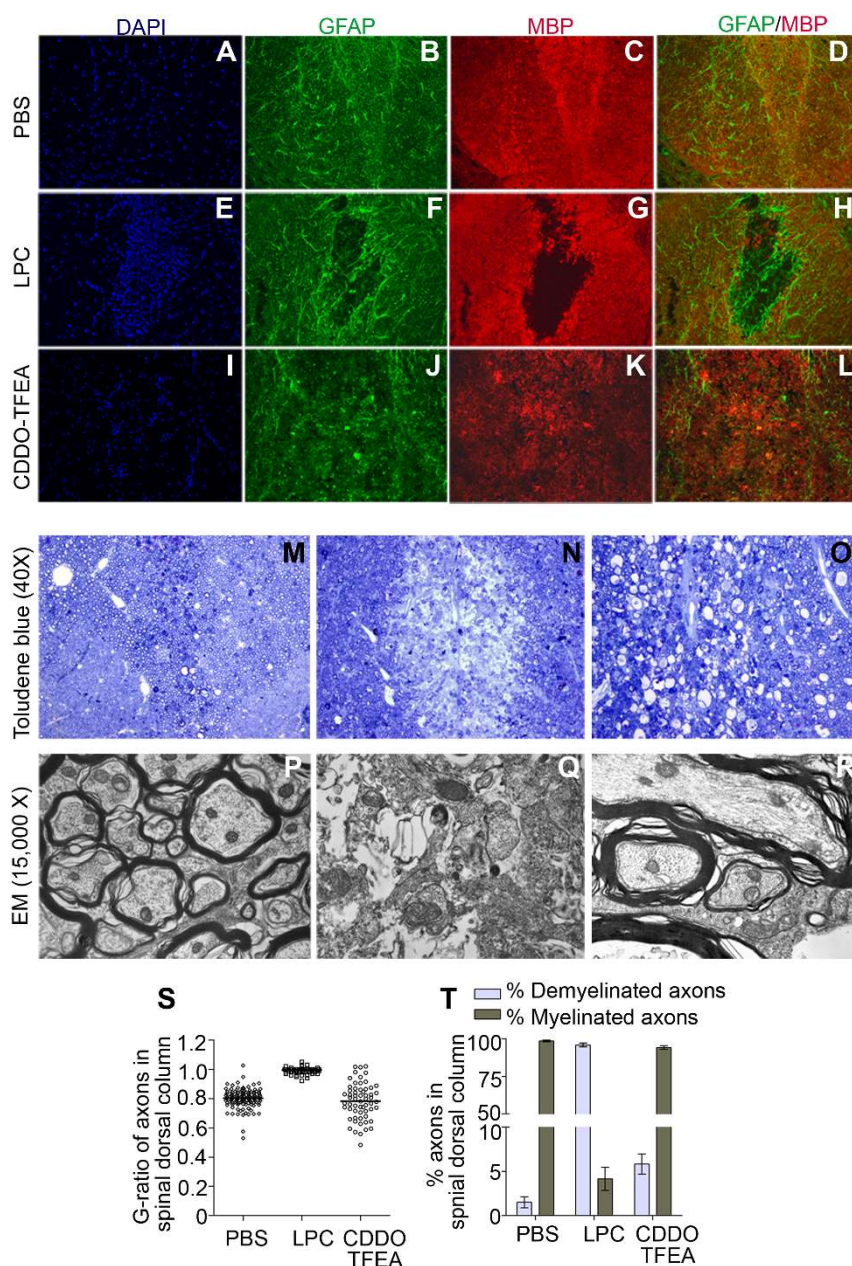


**Figure 6 | CDDO-TFEA is neuroprotective in the LPC-induced model of demyelination.** Immunostaining of tissue sections prepared from dorsal columns of the thoracic spinal cord of rats at the site of injection of either PBS (A–D) or LPC (E–H) or LPC+ CDDO-TFEA (I–L). Immunohistochemistry was performed with an anti-MBP antibody (for myelin), anti-GFAP antibody (for astrocytes) and anti-NG2 antibody (for oligodendrocytes). All images are taken at 200X magnification. Tissue sections prepared from spinal cord segments at sites injected either with LPC or LPC followed by CDDO-TFEA were subjected to toluidene blue staining (M–O) or electron microscopy (P–R) to analyze the myelin content in neurons at the site of each lesion. G-ratios of the axons in dorsal columns (S) and quantification of the percentage of demyelinated and myelinated axons in dorsal columns of spinal cord at the site of LPC injection (T) are shown here.

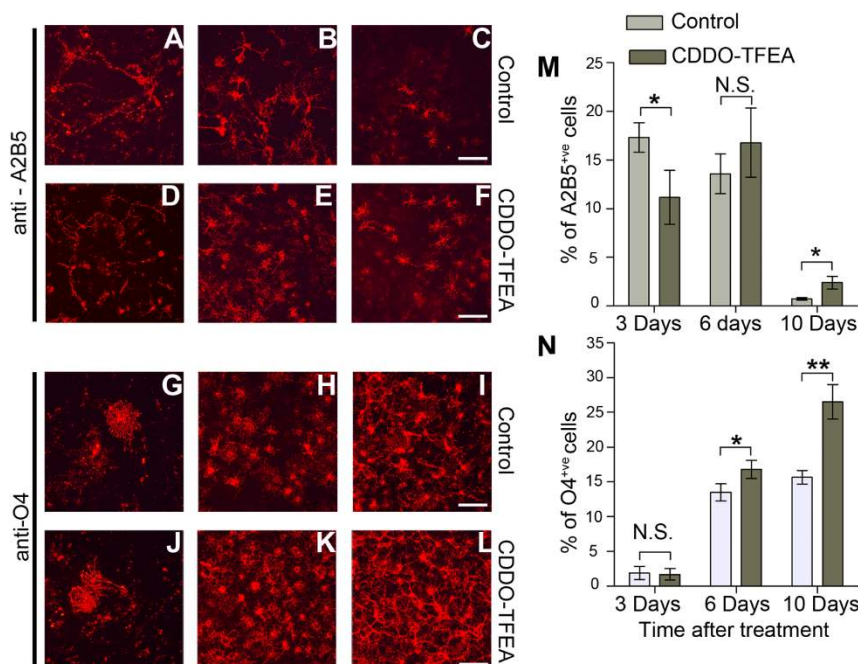


**Figure 7 | CDDO-TFEA induces early oligodendrocyte maturation.** Total brain cells prepared from P3 rat pups were cultured with vehicle (A–C and G–I) or with 10 nM CDDO-TFEA (D–F and J–L) for 3 days (A, D, G, J), 6 days (B, E, H, K), or 10 days (C, F, I, L). Cells were fixed and immunostained using antibodies against A2B5 to detect immature oligodendrocyte precursor cells (A–F) or against O4 to detect mature oligodendrocytes (G–L). (Scale bar is 100  $\mu$ m). Quantitative analysis of the percentage of (M) A2B5 or (N) O4 positive cells after different days of CDDO-TFEA treatment is shown. Data are the mean  $\pm$  SEM. \*\*, P, 0.01, \*, P, 0.05, Student's t test.

(Illumina Sentrix array Ref. 8v1.1) on lumbar spinal cord, directly comparing tissues collected from control mice and from mice following induction of EAE, with or without exposure to CDDO-TFEA. A total of 1433 genes were found to be differentially modulated in mice at the peak of EAE clinical scores compared to control mice (Fig. 8A). Among them, 135 genes known to be involved either in the cellular stress response or in inflammation were significantly altered by CDDO-TFEA treatment, and in most instances their expression returned to baseline (Fig. 8B–D). However, the induction of 11 $\beta$ -hydroxysteroid dehydrogenase type 1 (11bHSD1) and of prostaglandin D<sub>2</sub> synthase (PGDS) suggests that activation of steroid and prostaglandin biosynthetic pathways may contribute to the suppression of CNS inflammation by triterpenoids. We validated these gene array results by performing real time PCR on 9 different genes (Fig. 8E). The data suggest that inflammation driven suppression of both 11bHSD1 and of PGDS is reversed by exposure to CDDO-TFEA.

## Discussion

Multiple mechanisms operant in MS culminate ultimately in the generation of a highly oxidative microenvironment that is responsible for tissue injury and neurodegeneration<sup>44,45</sup>. The data presented here add to a growing body of literature that strongly support the clinical development of the family of natural and synthetic triterpenoids as chemopreventive and therapeutic agents in the context of neuro-inflammatory and neurodegenerative diseases, and specifically in the context of MS. While neuroprotective effects of administered exogenous antioxidants have been reported in EAE<sup>5,46</sup>, pursuit of strategies that employ newer agents such as synthetic triterpenoids to induce endogenous enzymatic antioxidants should be a more efficient means to inhibit the detrimental effects of ROS and thereby serve as an effective form of chemoprevention for MS.

Synthetic oleanane triterpenoids have emerged as a potent class of pharmacologic agents capable of strongly inducing the Nrf2-ARE axis, and this mechanism has been identified as playing a principal

role in the neuroprotective effects of CDDO derivatives in a variety of models of neurodegenerative disorders<sup>27</sup>. For example, in the murine SOD-1 model of Amyotrophic Lateral Sclerosis (ALS)<sup>47</sup>, exposure to CDDO-EA and CDDO-TFEA results in nuclear translocation of Nrf2 in cells expressing the SOD-1 mutant, and suppressed disease progression whether treatment was initiated in asymptomatic mice or at the onset of clinical manifestations. While the clinical response observed in the EAE model may be attributed to effects on Nrf2 expression and function, triterpenoids are multifunctional agents and it is quite likely that multiple targets participate in conferring protection in the setting of a complex neurodegenerative process like MS. For example, a role for Stat3 not only in the genesis of Th17 cells but also in the development of EAE has been defined<sup>48–50</sup>. Our laboratory and others have shown that Stat3 is a direct target of the synthetic triterpenoids<sup>28,51</sup>. Our demonstration that triterpenoid exposure following induction of EAE significantly represses both IL-17 mRNA and protein expression suggests that this mechanism may also contribute to the overall clinical response to triterpenoids in the EAE model.

It is noteworthy that the link between an induction of Hmox-1 and repression of the development of a Th17 response has also been demonstrated for other activators of Hmox-1 in preclinical models of EAE and inflammatory bowel disease (IBD). Hemin, a potent inducer of Hmox-1 and activator of Nrf2<sup>52</sup>, suppresses the development of IBD in mice exposed to dextran sodium sulfate (DSS) and this effect is also associated with a significant reduction in the production of IL-17<sup>53</sup>. Similarly, intraperitoneal administration of erythropoietin to MOG-EAE mice significantly reduced severity of disease in a manner that correlated with potent upregulation of Hmox-1 in the CNS and spleen and with a reduction of Th-17 T cell subsets<sup>54</sup>. Finally, the observation that IL-17 might act to directly suppress the expression of Hmox-1 in the context of an inflammatory response argues that the balance between these two factors may in fact be an important determinant of disease expression. Thus the unique capacity of triterpenoids to simultaneously repress IL-17

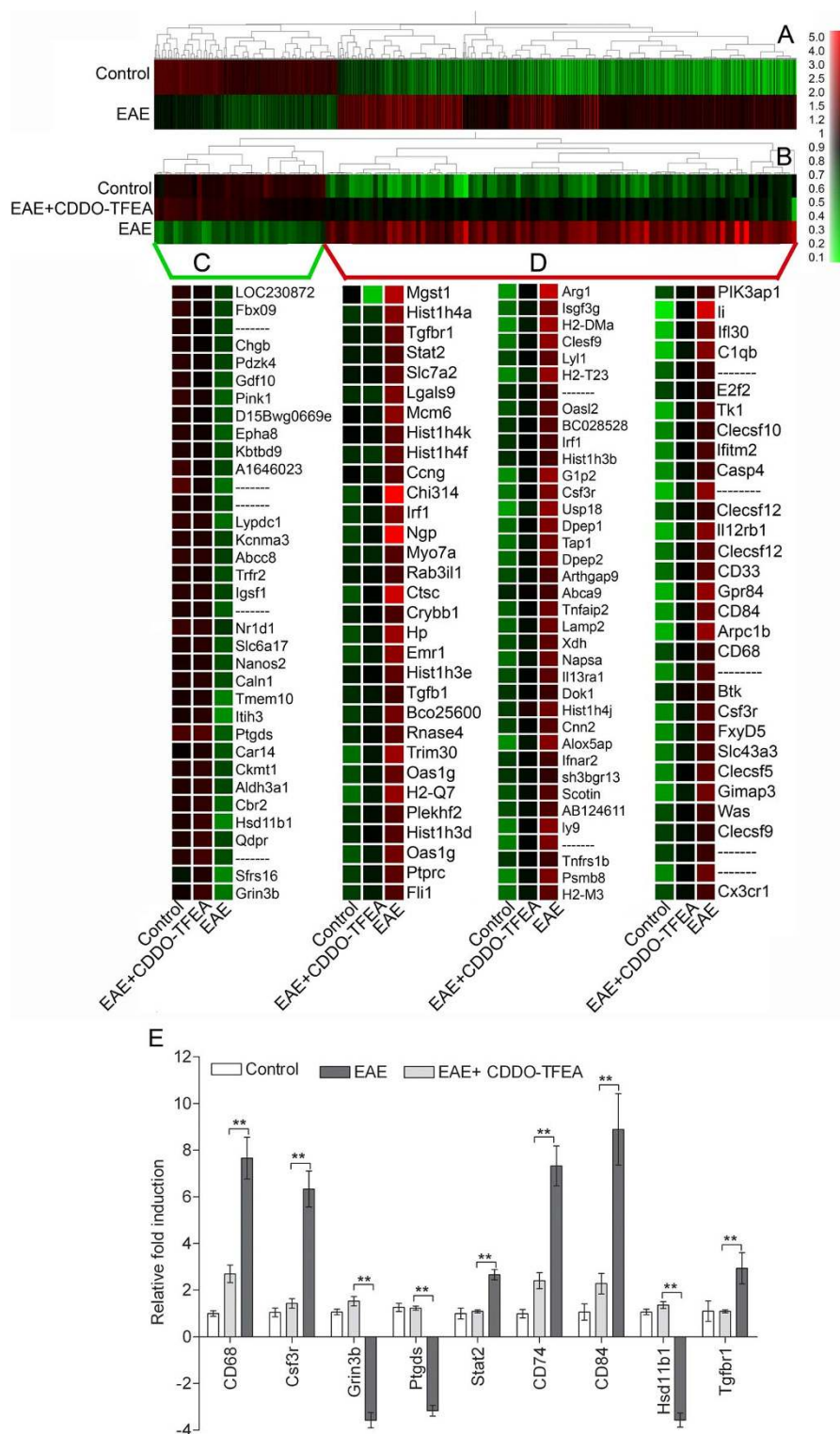


**Figure 8 | Microarray analysis of CNS tissues reveals global suppression of inflammatory genes by CDDO-TFEA in mice with EAE, with a concomitant induction of genes linked to resolution of inflammation.** Gene microarray analysis using Illumina Sentrix array Ref. 8v1.1, using mRNA collected from lumbar spinal cord of control mice and mice with EAE treated either with vehicle control or with CDDO-TFEA. (A) Heatmap of 1433 genes differentially expressed in EAE mice compared to control mice. (B) Heatmap of 135 genes significantly altered by CDDO-TFEA treatment. (C) Magnified heatmap (from panel B) of genes either down-regulated during EAE or (D) up-regulated during EAE, and their return to baseline after CDDO-TFEA treatment. (E) Quantitative PCR was performed using selected probes (as described in material method section) and RNA collected from affected CNS tissue of mice induced to develop EAE and treated with either CDDO-TFEA or vehicle control.  $\beta$ -actin levels were tested to normalize the amount of RNA and relative fold induction of transcript was calculated by comparing the basal level of expression of selected genes in normal mouse tissues. All data are the mean  $\pm$  SEM. \*\*,  $P < 0.01$ , Student's  $t$  test.





expression through inhibition of Stat3 and to activate HO-1 through Nrf-2 suggests their utility for treatment of MS.

It is intriguing to find the induction of both 11 $\beta$ -hydroxysteroid dehydrogenase type 1 (11bHSD1) and of prostaglandin D<sub>2</sub> synthase (PGDS) in the CNS in mice exposed to CDDO-TFEA. It has been suggested that a local deficit of cortisol in the CNS may underlie the relapsing-remitting nature of MS, perhaps secondary to poor local activation of cortisone via 11 $\beta$ -hydroxysteroid dehydrogenase type 1 (11bHSD1)<sup>55</sup>. MS patients have been found to maintain normal cortisol concentrations in serum yet exhibit lowered cortisol levels in the CSF during acute relapses. Although 11bHSD1 was not found to be expressed within active plaques, the significant induction in myelin-loaded macrophages *in vitro* suggests that production of this enzyme by infiltrating macrophages may contribute to the self-limiting nature of MS lesion development. Similarly, a reduction in the intrathecal synthesis of prostaglandin D<sub>2</sub> synthase (PGDS) has been documented during acute inflammatory demyelination<sup>56</sup>, and enhanced biosynthesis of prostaglandin (PG)D<sub>2</sub> and subsequent formation of 15-deoxy- $\Delta$ -PGJ<sub>2</sub> has been implicated in the resolution of inflammation<sup>57</sup>. It is intriguing that 15-PGJ<sub>2</sub> has been shown to activate Nrf2 signaling and to induce Hmox-1 in a manner similar to CDDO<sup>58</sup> thus demonstrating the capacity to contribute to the endogenous anti-oxidant response and raising the question whether the observed clinical response to triterpenoids shown here might reflect their capacity to mimic many of the functions of this endogenous anti-inflammatory protein.

Lastly, our data in the model of LPC-induced demyelination suggest that the efficacy of triterpenoids in the context of EAE is linked to a capacity to regulate astrocyte activation and to preserve CNS myelin. Nrf-2<sup>-/-</sup> mice develop a spontaneous progressive leukoencephalopathy, with vacuolar degeneration that is linked to myelin unwinding, intramyelinic cysts and oxidative damage to myelin<sup>10</sup>. Similarly, the observation that the anti-oxidant fumaric acid (FA) can preserve myelin and axonal density has also been linked to the capacity of FA and its esters to regulate Nrf-2 activity, and may be a mechanism contributing to the observed reduction of gadolinium enhancing lesions in MS patients treated with dimethylfumarate<sup>59</sup>. Indeed, the beneficial effects of dimethylfumarate for axon preservation and astrocyte activation in the MOG-EAE model are lost in mice deficient in Nrf-2 gene expression<sup>60</sup>.

In conclusion, the data present here demonstrate the efficacy of multifunctional triterpenoids in suppressing clinical and pathologic features of disease in preclinical models of MS. These small molecules have a unique capacity to simultaneously target intermediates that drive production of disease-inducing cytokines, such as IL-17, while inducing neuroprotective pathways activated through Nrf-2. Thus, synthetic triterpenoids may serve as both therapeutic and chemopreventive agents in the context of neurodegenerative and inflammatory diseases affecting the CNS.

## Methods

**Animals.** C57BL/6 and SJL female mice (for EAE studies) and male Wistar rats (for LPC studies) were housed in a pathogen free animal facility in standard cages with free access to food and water in climate and light controlled rooms. All experimental procedures were approved by the Animal Care and Use Committee of the Case Western Reserve University.

**EAE induction.** EAE was induced in 10–12 weeks old, age matched female mice by subcutaneous immunization on both flanks with 200  $\mu$ l of emulsion containing either Complete Freund's adjuvant (100  $\mu$ l of incomplete Freund's adjuvant with 8 mg/ml of *Mycobacterium Tuberculosis* and 100  $\mu$ l of PBS) (DIFCO Laboratories) or Complete Freund's adjuvant with 200  $\mu$ g of MOG (35–55). At the time of injection and 48 hours later 200 ng of pertussis toxin (List Biological Laboratories) was injected intraperitoneally in 100  $\mu$ l of PBS. Mice were monitored for daily clinical signs of EAE and the following criteria were used to grade clinical scores: 0-no signs of disease;

1-limp tail; 2-moderate hind-limb weakness; 3-severe hind-limb weakness; 4-Complete hind limb paralysis; 5- quadriplegia or premoribund state; 6-death.

**Drug treatment.** CDDO-Me, CDDO-EA or CDDO-TFEA were dissolved in a minimal amount of DMSO to obtain 10 mM stock and further dissolved in 7.5% PBST (7.5 ml Tween-80 dissolved in 100 ml of PBS) to obtain a final concentration of 100 nM. Animals were injected with 100  $\mu$ l of this solution by intra-peritoneal (i.p.) injection at the interval of 48 hours for a total of 5 injections. Therapy was initiated in mice with varying severity of disease as noted by different clinical scores, starting after 15 days of MOG-35-55 immunization. Control animals were injected with a similar volume of vehicle i.e. 7.5% PBST.

**Histology and immunohistochemistry.** On day 18 to 23 (at clinical scores 4 to 5 in control mice with EAE) and at clinical score 0 in recipients of CDDO-TFEA treatment, mice were anesthetized and perfused with phosphate buffer saline (PBS) followed with 4% paraformaldehyde in PBS (PFA-PBS). Brain and spinal cord were collected and fixed in 4% PFA-PBS and embedded in paraffin to obtain 5  $\mu$ m thick sections. At least 10 to 12 serial sections were obtained from 4 different regions of the brain (rostral cerebrum, mid cerebrum, mid brain and cerebellum with brain stem). Spinal cord was divided into 3 parts (cervical, thoracic and lumbar). At least 5 sections from each part and longitudinal serial sections of all regions were obtained for representation of the entire spinal cord. Tissue sections were stained with hematoxylin & eosin (H&E) to assess routine histology and inflammation and also with Luxol Fast Blue and the Periodic Acid Schiff reagent to analyze myelin content. Each section was assigned a histological score for inflammation and demyelination from 0 to 3 by an observer blinded to sample identity, where 0 represents no lesions, 1- moderate and 3 represents severe lesions. Spinal cord sections were immunostained with anti myeloperoxidase antibody to detect granulocytes infiltration and anti-F4/80 antibody for macrophage and microglia.

**Western blot analysis.** Animals were sacrificed for tissue collection at different time points after immunization and drug treatment. Brain (further divided into forebrain, midbrain and hindbrain) and spinal cord (further divided into cervical, thoracic and lumbar) were collected and snap frozen. Tissue homogenates were prepared in lysis buffer, consisting of T-PER, tissue protein extraction reagent (Pierce, Rockford, IL), a protease inhibitor cocktail tablet (Roche, Mannheim, Germany) and 1 : 100 diluted phosphatase inhibitor mixtures I and II (Sigma, St. Louis, MO). Proteins were denatured and equal amounts of proteins were electrophoresed in 4–12% bis-Tris/polyacrylamide gels (NuPAGE; Invitrogen, Carlsbad, CA) and transferred to nitrocellulose membranes with 0.2  $\mu$ m pores (Invitrogen). The membranes were blocked for 2 h in blocking solution (TBS containing 10% nonfat dry milk and 0.05% Tween 20) and incubated overnight at 4°C with primary antibody diluted in blocking solution. Incubation with horseradish peroxidase-conjugated secondary antibody was performed at room temperature for 1 h, and immunoreactivity was detected by using enhanced chemiluminescence (Pierce, Rockford, IL).

**Oligodendrocyte primary culture.** Dissociated brain cultures were made from Sprague-Dawley rat pups at postnatal day 3, plated on poly-L-lysine/Laminin coated coverslips and grown in 1% fetal bovine serum in DMEM supplemented with GlutaMAX<sup>TM</sup>, Penicillin-Streptomycin, Hong's N2 and PDGF-AA. Treatment with vehicle (control) or vehicle + 10 nM CDDO-TFEA began one day after dissociation and lasted for three, six or ten days *in vitro*. Immunocytochemical markers of the oligodendrocyte lineages were assayed, including A2B5 (for immature oligodendrocyte precursor cells), and O4, (for mature marker of oligodendrocyte precursor cells). A total of 100 to 300 total cells were counted from five different areas in each culture and positive immunoreactive cells for A2B5 or O4 were plotted as percentage of total cells.

**Antibodies.** The rabbit polyclonal anti-iNOS and anti-Hmox-1 (Santa Cruz Biotechnology, Santa Cruz, CA) were used for Western blot analysis (1 : 200). For immunohistochemistry 2  $\mu$ g/ml of rabbit polyclonal anti-myeloperoxidase (lot 373A603A (1); Lab Vision; Fremont, CA), or 10  $\mu$ g/ml of the rat IgG2b MAb F4/80 (clone C1:A3-1; Serotec; Raleigh, NC) were used. Secondary horseradishperoxidase-conjugated antibodies were obtained from AmershamBiosciences (Piscataway, NJ) and used at 1 : 2000 dilution for immunoblots analysis and 2.5  $\mu$ g/ml biotinylated rabbit anti-rat IgG secondary antibody (Vector Laboratories; Burlingame, CA) to detect F4/80 and 2.5  $\mu$ g/ml biotinylated goat anti-rabbit IgG secondary antibody (Vector) to detect myeloperoxidase.

**ELISA.** Serum levels of IL-2, IL-4, IL-6, GM-CSF, TNF and IFN- $\gamma$  were detected with OptiEIA Elisa sets (BD Biosciences and IL-17 was detected with DuoSet ELISA development System (R&D systems) as per manufacturer's suggested protocol.

**Ex vivo restimulation of T cells.** Mice immunized with or without MOG(35-55) (clinical score-5) or CDDO-TFEA treated (clinical score-0) were sacrificed and a single cell suspension was prepared from draining lymph nodes (Inguinal and brachial) and restimulated with 33  $\mu$ g/ml of MOG (35–55) in presence or absence of CDDO-TFEA and 50 ng/ml mIL7. Cells were seeded in a 96 well plate at a density of  $2 \times 10^5$ . After 72 hours culture supernatants were collected for analysis of cytokine secretion and cells were used for RNA preparation. For proliferation assays, 0.5  $\mu$ ci of (<sup>3</sup>H) thymidine was added in cultures during last 12 hours and thymidine incorporation was measured as cell proliferation.



Table 1 | Quantitative PCR probes

Genes of interest	Assay ID*	Common Name
IL-17 $\alpha$	Mm00439619_m1	interleukin 17A
NOS-2	Mm01309902_m1	Nitric oxide synthase 2
IFN- $\gamma$	Mm99999071_m1	hemoxygenase 1
Hmox-1	Mm00516007_m1	interferon gamma
Nrf-2	Mm03053465_s1	nuclear receptor subfamily 2, group F, member 2
Ptgds	Mm01330614_g1	PGD2; PGDS
Grin3b	Mm00504568_m1	NR3B
Stat2	Mm00490880_m1	AW496480
Cd68	Mm00839636_g1	gp110; Scard1
Csf3r	Mm00432735_m1	Cd114; Csfgr; G-CSFR
Tgfb $\beta$ 1	Mm00436971_m1	ALK5; Alk-5; TbetaR1
Hsd11b1	Mm00476182_m1	Hsd11b1
Cd74	Mm00658576_m1	li; CLIP; DHLAG
Cd84	Mm00488934_m1	CDw84; SLAMF5
$\beta$ -Actin	Mm00607939_s1	

**LPC induced demyelination.** Three to four months old male Wistar rats were used for this study. Demyelination in the spinal cord was induced by LPC injection as described previously<sup>30</sup> with subtle modification in protocol. In brief, animals were anesthetized with 5 ml per kg of body weight of 0.2 ml ketamine (Fort Dodge), 0.1 ml xylazine (Lloyd Laboratories) and 0.7 ml of distilled water. After shaving and cleaning with ethanol and betadine, a T10 laminectomy was performed in a stereotactic apparatus (Stoelting). Using a 30-mm glass micropipette attached to a Nano-injector (World Precision Instruments), 1.5  $\mu$ l of 1% freshly prepared LPC (Sigma) solution was infused at 15 ml/hour. The needle was kept in place for 5 min to prevent reflux; the skin was closed and treated with Betagen (Med-Pharmex). In order to rule out any mechanical injury control rats were subjected to similar surgical process but in spite of LPC similar volume of PBS was injected. Rats received either 10 nM CDDO-TFEA or vehicle control at the time of LPC injection and again after 48 hours at the site of LPC injection. After 7 days all animals were sacrificed and targeted spinal cord tissue was collected and processed for electron microscopy (for analyzing the myelin content) and frozen tissue sections were used for immunostaining to analyze myelin content and recruitment of oligodendrocyte and glial cells at the site of injury.

**Electron microscopy.** We anesthetized and perfused the animals with Sorenson's buffer followed by solution containing 4% paraformaldehyde (wt/vol) and 2.5% glutaraldehyde (vol/vol). Spinal cords were sliced into 1–2-mm sections and post-fixed in the same solution overnight at 4°C, after which sections were embedded in Araldite resin. Semi-thin sections were stained with 1% Toluidine blue staining (wt/vol) at 65°C for a few seconds, washed several times with water and then dehydrated and mounted with Permount. Thin sections were cut, stained with uranyl acetate and lead citrate and analyzed. G ratios (defined as the diameter of the axon divided by the diameter of the axon and myelin) were calculated from the outer perimeter of the axon divided by the total perimeter of the axon and myelin. Six pictures were randomly chosen for each mouse and 100–200 fibers per picture were calculated. At least 6 mice per strain per time point were analyzed. The data are shown as G ratio and total number of myelinated fibers.

**Oligonucleotide microarray analysis.** Total RNA was isolated using Trizol reagent (Invitrogen) and RNeasy (Qiagen) from control and EAE mice lumbar spinal cord, treated with or without CDDO-TFEA. Each tissue sample was derived from a different individual mouse giving three true biological replicate samples. The yield was quantified using NanoDrop ND-1000 Spectrophotometer (Nanodrop Technologies, Delaware) and quality checked by conventional denaturing 1% agarose gel analysis. For microarray analysis, extracted total RNA was biotinylated and amplified using the Illumina® TotalPrep RNA Amplification Kit. Labeled cRNA was then hybridized with IlluminaSentrix® array (Sentrix Mouse Ref 8v1.1) according to their standard protocol (Illumina). Following hybridization and washing, arrays were scanned using IlluminaBeadStudio (version 3.1). The raw data from all the arrays were then exported out and analyzed using GeneSpring 7.3.1 (Agilent Technologies). Expression of all genes on a chip was normalized globally to the expression value of the median of the chip and each gene normalized across conditions to a median of 1.0. This approach reduced the expression ratio for every gene in each of the control samples to 1 and set the expression ratio for each gene in each test sample to a value indicative of its expression relative to that in the corresponding control. The normalized data were then filtered by volcano plot to identify genes whose expression (in all three biological replicates) appears to be up- or down- regulated by an arbitrary cutoff of at least 1.5 fold with p-value = 0.05. Statistical analysis was performed on the log expression ratios utilizing one way Students t-test analysis of variance without any multiple testing correction. No post-hoc analysis was applied.

**Quantitative Real-time polymerase chain reaction.** 10  $\mu$ l of total RNA (2 micrograms) from each sample were reverse transcribed using High-Capacity

cDNA Reverse Transcription Kits (Applied Biosystems) that contains 10X RT Buffer; 25X dNTP Mix (100 mM); 10RT Random Primers; Multiscribe™; Reverse Transcriptase and nuclease-free water in a final volume of 20  $\mu$ l reaction mixture. Reverse transcription was performed using the following program on a thermal cycler (Applied Biosystems) using only 1 cycle: (step 1) at 25°C for 10 min; (step 2) at 37°C for 120 min; (step 3) at 85°C for 5 sec; and (step 4) at 4°C for infinity. QRT-PCR was performed with an ABI 7500 system (Applied Biosystems) to validate the microarray results on a number of genes apparently exhibiting differential expression. Pre-synthesized primers specific for the genes purchased from ABI are shown in Table 1.

- Noseworthy, J. H., Lucchinetti, C., Rodriguez, M. & Weinshenker, B. G. Multiple sclerosis. *N Engl J Med* **343**, 938–952 (2000).
- Gutcher, I., et al. Autocrine transforming growth factor-beta1 promotes in vivo Th17 cell differentiation. *Immunity* **34**, 396–408 (2011).
- Benveniste, E. N. Cytokine actions in the central nervous system. *Cytokine Growth Factor Rev* **9**, 259–275 (1998).
- Ruuls, S. R., et al. Reactive oxygen species are involved in the pathogenesis of experimental allergic encephalomyelitis in Lewis rats. *J Neuroimmunol* **56**, 207–217 (1995).
- Gilgun-Sherki, Y., Melamed, E. & Offen, D. The role of oxidative stress in the pathogenesis of multiple sclerosis: the need for effective antioxidant therapy. *J Neurol* **251**, 261–268 (2004).
- Smith, K. J., Kapoor, R. & Felts, P. A. Demyelination: the role of reactive oxygen and nitrogen species. *Brain Pathol* **9**, 69–92 (1999).
- van Meeteren, M. E., Teunissen, C. E., Dijkstra, C. D. & van Tol, E. A. Antioxidants and polyunsaturated fatty acids in multiple sclerosis. *Eur J Clin Nutr* **59**, 1347–1361 (2005).
- Johnson, D. A., Amirahmadi, S., Ward, C., Fabry, Z. & Johnson, J. A. The absence of the pro-antioxidant transcription factor Nrf2 exacerbates experimental autoimmune encephalomyelitis. *Toxicol Sci* **114**, 237–246 (2010).
- Innamorato, N. G., et al. The transcription factor Nrf2 is a therapeutic target against brain inflammation. *J Immunol* **181**, 680–689 (2008).
- Hubbs, A. F., et al. Vacuolar leukoencephalopathy with widespread astrogliosis in mice lacking transcription factor Nrf2. *Am J Pathol* **170**, 2068–2076 (2007).
- Tajouri, L., et al. Quantitative and qualitative changes in gene expression patterns characterize the activity of plaques in multiple sclerosis. *Brain Res Mol Brain Res* **119**, 170–183 (2003).
- Guy, J., Qi, X. & Hauswirth, W. W. Adeno-associated viral-mediated catalase expression suppresses optic neuritis in experimental allergic encephalomyelitis. *Proc Natl Acad Sci U S A* **95**, 13847–13852 (1998).
- Singh, I., et al. Impaired peroxisomal function in the central nervous system with inflammatory disease of experimental autoimmune encephalomyelitis animals and protection by lovastatin treatment. *Brain Res* **1022**, 1–11 (2004).
- Liu, Y., Liu, J., Tetzlaff, W., Paty, D. W. & Cynader, M. S. Biliverdin reductase, a major physiologic cytoprotectant, suppresses experimental autoimmune encephalomyelitis. *Free Radic Biol Med* **40**, 960–967 (2006).
- Liu, Y., et al. Heme oxygenase-1 plays an important protective role in experimental autoimmune encephalomyelitis. *Neuroreport* **12**, 1841–1845 (2001).
- Connolly, J. D. & Hill, R. A. Triterpenoids. *Nat Prod Rep* **18**, 560–578 (2001).
- Xu, R., Fazio, G. C. & Matsuda, S. P. On the origins of triterpenoid skeletal diversity. *Phytochemistry* **65**, 261–291 (2004).
- Dzubak, P., et al. Pharmacological activities of natural triterpenoids and their therapeutic implications. *Nat Prod Rep* **23**, 394–411 (2006).
- Liu, J. Oleanolic acid and ursolic acid: research perspectives. *J Ethnopharmacol* **100**, 92–94 (2005).



20. Raphael, T. J. & Kuttan, G. Effect of naturally occurring triterpenoids glycyrrhizic acid, ursolic acid, oleanolic acid and nomilin on the immune system. *Phytomedicine* **10**, 483–489 (2003).
21. Martin, R., *et al.* Beneficial actions of oleanolic acid in an experimental model of multiple sclerosis: a potential therapeutic role. *Biochem Pharmacol* **79**, 198–208 (2010).
22. Tran, T. A., McCoy, M. K., Sporn, M. B. & Tansey, M. G. The synthetic triterpenoid CDDO-methyl ester modulates microglial activities, inhibits TNF production, and provides dopaminergic neuroprotection. *J Neuroinflammation* **5**, 14 (2008).
23. Pergola, P. E., *et al.* Effect of bardoxolone methyl on kidney function in patients with T2D and Stage 3b–4 CKD. *Am J Nephrol* **33**, 469–476 (2011).
24. Pergola, P. E., *et al.* Bardoxolone methyl and kidney function in CKD with type 2 diabetes. *N Engl J Med* **365**, 327–336 (2011).
25. Dumont, M., *et al.* Triterpenoid CDDO-methylamide improves memory and decreases amyloid plaques in a transgenic mouse model of Alzheimer's disease. *J Neurochem* **109**, 502–512 (2009).
26. Liby, K. T., Yore, M. M. & Sporn, M. B. Triterpenoids and rexinoids as multifunctional agents for the prevention and treatment of cancer. *Nat Rev Cancer* **7**, 357–369 (2007).
27. Stack, C., *et al.* Triterpenoids CDDO-ethyl amide and CDDO-trifluoroethyl amide improve the behavioral phenotype and brain pathology in a transgenic mouse model of Huntington's disease. *Free Radic Biol Med* **49**, 147–158 (2010).
28. Liby, K., *et al.* The synthetic triterpenoid CDDO-Imidazole suppresses STAT phosphorylation and induces apoptosis in myeloma and lung cancer cells. *Clin Cancer Res* **12**, 4288–4293 (2006).
29. Yore, M. M., Liby, K. T., Honda, T., Gribble, G. W. & Sporn, M. B. The synthetic triterpenoid 1-[2-cyano-3,12-dioxooleana-1,9(11)-dien-28-oyl]imidazole blocks nuclear factor-kappaB activation through direct inhibition of IkbkappaB kinase beta. *Mol Cancer Ther* **5**, 3232–3239 (2006).
30. Bayer, A. L., Lee, J. Y., de la Barrera, A., Surh, C. D. & Malek, T. R. A function for IL-7R for CD4+CD25+Foxp3+ T regulatory cells. *J Immunol* **181**, 225–234 (2008).
31. Lundmark, F., *et al.* Variation in interleukin 7 receptor alpha chain (IL7R) influences risk of multiple sclerosis. *Nat Genet* **39**, 1108–1113 (2007).
32. Cross, A. H., *et al.* Inducible nitric oxide synthase gene expression and enzyme activity correlate with disease activity in murine experimental autoimmune encephalomyelitis. *J Neuroimmunol* **71**, 145–153 (1996).
33. Koprowski, H., *et al.* In vivo expression of inducible nitric oxide synthase in experimentally induced neurologic diseases. *Proc Natl Acad Sci U S A* **90**, 3024–3027 (1993).
34. Lin, R. F., Lin, T. S., Tilton, R. G. & Cross, A. H. Nitric oxide localized to spinal cords of mice with experimental allergic encephalomyelitis: an electron paramagnetic resonance study. *J Exp Med* **178**, 643–648 (1993).
35. Okuda, Y., *et al.* Expression of the inducible isoform of nitric oxide synthase in the central nervous system of mice correlates with the severity of actively induced experimental allergic encephalomyelitis. *J Neuroimmunol* **62**, 103–112 (1995).
36. Xie, Q. & Nathan, C. The high-output nitric oxide pathway: role and regulation. *J Leukoc Biol* **56**, 576–582 (1994).
37. Henry, Y., *et al.* Nitric oxide, a biological effector. Electron paramagnetic resonance detection of nitrosyl-iron-protein complexes in whole cells. *Eur Biophys J* **20**, 1–15 (1991).
38. Ialenti, A., Iannaro, A., Monaco, S. & Di Rosa, M. Modulation of acute inflammation by endogenous nitric oxide. *Eur J Pharmacol* **211**, 177–182 (1992).
39. Chora, A. A., *et al.* Heme oxygenase-1 and carbon monoxide suppress autoimmune neuroinflammation. *J Clin Invest* **117**, 438–447 (2007).
40. Chen, Y., *et al.* Anti-IL-23 therapy inhibits multiple inflammatory pathways and ameliorates autoimmune encephalomyelitis. *J Clin Invest* **116**, 1317–1326 (2006).
41. Hofstetter, H. H., *et al.* Therapeutic efficacy of IL-17 neutralization in murine experimental autoimmune encephalomyelitis. *Cell Immunol* **237**, 123–130 (2005).
42. Smith, K. J. & McDonald, W. I. Spontaneous and mechanically evoked activity due to central demyelinating lesion. *Nature* **286**, 154–155 (1980).
43. Fuller, M. L., *et al.* Bone morphogenetic proteins promote gliosis in demyelinating spinal cord lesions. *Ann Neurol* **62**, 288–300 (2007).
44. Gonsette, R. E. Oxidative stress and excitotoxicity: a therapeutic issue in multiple sclerosis? *Mult Scler* **14**, 22–34 (2008).
45. Witherick, J., Wilkins, A., Scolding, N. & Kemp, K. Mechanisms of oxidative damage in multiple sclerosis and a cell therapy approach to treatment. *Autoimmune Dis* **2011**, 164608 (2010).
46. van Meeteren, M. E., Hendriks, J. J., Dijkstra, C. D. & van Tol, E. A. Dietary compounds prevent oxidative damage and nitric oxide production by cells involved in demyelinating disease. *Biochem Pharmacol* **67**, 967–975 (2004).
47. Neymotin, A., *et al.* Neuroprotective effect of Nrf2/ARE activators, CDDO ethylamide and CDDO trifluoroethylamide, in a mouse model of amyotrophic lateral sclerosis. *Free Radic Biol Med* **51**, 88–96 (2011).
48. Jaidi-Niaragh, F. & Mirshafiey, A. Th17 cell, the new player of neuroinflammatory process in multiple sclerosis. *Scand J Immunol* **74**, 1–13 (2011).
49. Jin, W., Zhou, X. F., Yu, J., Cheng, X. & Sun, S. C. Regulation of Th17 cell differentiation and EAE induction by MAP3K NIK. *Blood* **113**, 6603–6610 (2009).
50. Ogura, H., *et al.* Interleukin-17 promotes autoimmunity by triggering a positive-feedback loop via interleukin-6 induction. *Immunity* **29**, 628–636 (2008).
51. Ahmad, R., Raina, D., Meyer, C. & Kufe, D. Triterpenoid CDDO-methyl ester inhibits the Janus-activated kinase-1 (JAK1)->signal transducer and activator of transcription-3 (STAT3) pathway by direct inhibition of JAK1 and STAT3. *Cancer Res* **68**, 2920–2926 (2008).
52. Kim, Y. C., *et al.* Hemin-induced activation of the thioredoxin gene by Nrf2. A differential regulation of the antioxidant responsive element by a switch of its binding factors. *J Biol Chem* **276**, 18399–18406 (2001).
53. Zhong, W., *et al.* Hemin exerts multiple protective mechanisms and attenuates dextran sulfate sodium-induced colitis. *J Pediatr Gastroenterol Nutr* **50**, 132–139 (2010).
54. Chen, S. J., *et al.* Erythropoietin enhances endogenous haem oxygenase-1 and represses immune responses to ameliorate experimental autoimmune encephalomyelitis. *Clin Exp Immunol* **162**, 210–223 (2010).
55. Heidbrink, C., *et al.* Reduced cortisol levels in cerebrospinal fluid and differential distribution of 11beta-hydroxysteroid dehydrogenases in multiple sclerosis: implications for lesion pathogenesis. *Brain Behav Immun* **24**, 975–984 (2010).
56. Huang, Y. C., *et al.* Decreased intrathecal synthesis of prostaglandin D2 synthase in the cerebrospinal fluid of patients with acute inflammatory demyelinating polyneuropathy. *J Neuroimmunol* **206**, 100–105 (2009).
57. Rajakari, R., *et al.* Hematopoietic prostaglandin D2 synthase controls the onset and resolution of acute inflammation through PGD2 and 15-deoxyDelta12 14 PGJ2. *Proc Natl Acad Sci U S A* **104**, 20979–20984 (2007).
58. Ikeda, Y., *et al.* Suppression of rat thromboxane synthase gene transcription by peroxisome proliferator-activated receptor gamma in macrophages via an interaction with NRF2. *J Biol Chem* **275**, 33142–33150 (2000).
59. Gold, R., Linker, R. A. & Stangel, M. Fumaric acid and its esters: An emerging treatment for multiple sclerosis with antioxidative mechanism of action. *Clin Immunol* (2011).
60. Linker, R. A., *et al.* Fumaric acid esters exert neuroprotective effects in neuroinflammation via activation of the Nrf2 antioxidant pathway. *Brain* **134**, 678–692 (2011).

## Acknowledgments

We are thankful to Janet Robinson and Jennifer Alabran for their expert technical support and helpful discussions. We also thank NUS, Singapore for providing travel support for Dr. Pareek. This work was supported by the intramural funds from CWRU and The Case Research Institute. Dr. Letterio would like to thank Jane and Lee Seidman for their support through their endowment for Pediatric Cancer Innovation.

## Authors contribution

J.J.L. and T.K.P. conceived and coordinated the study, designed the experiments, analyzed the data and wrote the manuscript, T.K.P. carried out major biochemical and biological experiments, A.B. carried out LPC studies, S.K. and S.L.L. performed and analyzed microarray experiments, A.Z. carried out OPC maturation experiments, L.B. helped with PLP-EAE experiments, M.L.C. performed histopathological analyses, C.M., K.T.L., R.H.M., M.B.S., T.K.P. and J.J.L. discussed the hypothesis and interpreted the data.

## Additional information

**Supplementary information** accompanies this paper at <http://www.nature.com/scientificreports>

**Competing financial interests:** A patent application (US 2009/0060873/A1) is pending related to use of synthetic triterpenoids in treatment of multiple sclerosis.

**License:** This work is licensed under a Creative Commons Attribution-NonCommercial-ShareAlike 3.0 Unported License. To view a copy of this license, visit <http://creativecommons.org/licenses/by-nc-sa/3.0/>

**How to cite this article:** Pareek, T.K. *et al.* Triterpenoid modulation of IL-17 and Nrf-2 expression ameliorates neuroinflammation and promotes remyelination in autoimmune encephalomyelitis. *Sci. Rep.* **1**, 201; DOI:10.1038/srep00201 (2011).